Numerical Investigation of Hydromagnetic Effect on the Natural Convection Heat Transfer from Circular Cylinder in an Enclosed Enclosure

Omar **M**ohammed **A**li
Department of mechanics, College of Engineering, University of Zakho, Kurdistan Region, Iraq.

(Accepted for publication: December 21, 2016)

Abstract:

The natural convection heat transfer from horizontal circular cylinder placed in a square enclosure is investigated numerically. The study deals with the effect of magnetic field on the flow and heat transfer characteristics. The investigation employs different Hartman numbers (0, 50, 100, 200), different Rayleigh numbers (10^3, 10^4, and 10^5) with constant enclosure width to cylinder diameter ratios W/D = 2.5. The study included the solving of the governing equations in the form of the vorticity-stream function to be fitted with coordinate system. The algebraic grid generation is used to generate initial transformation. The elliptic grid generation is used to fit with physical domain between the heated horizontal cylinder and the enclosure into a computational domain. The resulting equations are solved using finite difference method that based on the finite volume.

The research studied the influence of the variation the Hartman number on the local and average Nusselt numbers, flow patterns and temperature distributions with different Rayleigh numbers. The effect of Hartman numbers on the flow patterns and temperature distributions will be displayed using streamlines and isotherms.

The results show that the conduction heat transfer is the dominant mode for low Rayleigh numbers. The convection heat transfer is the dominant mode of the heat transfer for high Rayleigh number in absence of the magnetic effect. The convection heat transfer convert to conduction mode at high Rayleigh numbers due to the effect of the magnetic field in the fluid. Also, the results show that the behavior of the local Nusselt numbers for Ha = 0 are unique and differ from those of other higher Hartman numbers for all Rayleigh numbers.

Keywords*: Heat Transfer, Circular Cylinder, Square Enclosure, Numerical.*

NOMENCLATURE

Symbol	Definition	Unit
Nu	Average Nusselt number, (h.D/k).	
D	Cylinder diameter.	m
$d_{i,j}$	Source term in the general equation, eqn. (12).	
h	Convective heat transfer coefficient.	$W/m^2.°C$
J	Jacobian.	
K	Thermal conductivity of the air.	W/m.°C
p	Pressure.	N/m^2
P	Coordinate control function.	
Pr	Prandtl number, (ν/α).	
Q	Coordinate control function.	
R	maximum absolute residual value.	
Ra	Rayleigh number, $(g\beta\Delta TD^3/\nu\alpha)$.	
t	Time.	seconds
T	Temperature.	°C
u	Velocity in x-direction.	m/s
v	Velocity in y-direction.	m/s
W	Enclosure Width.	cm
W	Relaxation factor.	
x	Horizontal direction in physical domain.	m
X	Dimensionless horizontal direction in physical domain.	
y	Vertical direction in physical domain.	m
Y	Dimensionless vertical direction in physical domain.	

	Greek Symbols	
ΔT	Difference between cylinder surface temperature and environmental temperature.	°C
μ	Viscosity of the air.	kg/m.s
β	Coefficient of thermal expansion.	1/°C
η	Vertical direction in computational domain.	
ξ	Horizontal direction in computational domain.	
Ψ	Dimensionless stream function.	
ω	Vorticity.	1/s
ϖ	Dimensionless vorticity.	
υ	Kinematic viscosity.	m^2/s
θ	Dimensionless temperature.	
ϕ	Dependent variable.	
ψ	Stream Function.	1/sec.
	Subscript	
S	Cylinder surface.	
∞	Environment.	
X	Derivative in x-direction.	
Y	Derivative in y-direction.	
ξ	Derivative in ξ-direction.	
D	Circular cylinder diameter.	
ψ	Stream function.	
T	Temperature.	
ω	Vorticity	

Introduction

The natural convection heat transfer from cylinder in the enclosed space is very important because of its wide applications in the industrial such as in thermal storage system, and cooling systems in nuclear reactors, cooling of electronic equipment, etc. The effect of hydromagnetic on the natural convection heat transfer is of great importance in many industrial applications such as crystal growth in liquid, cooling of nuclear reactor, electronic package, microelectronic devices, and solar technology. There are two body forces in the natural convection under the influence of the magnetic field: buoyancy force and Lorentz force. The two forces interact with each other and has an effect on the heat and mass transfer, Sheikholeslami et. al., 2013.

There are large numbers of literatures published in the past decades. Mudhaf et. al., 2004 studied numerically steady, laminar, natural convective flow of electrically conducting liquid metals such as gallium and germanium in an inclined rectangular enclosure in the presence of a uniform magnetic field. Transverse gradient of heat is applied on two opposing walls of the inclined enclosure while the other two walls are adiabatic. A magnetic field is applied normally to the non-insulated walls. A numerical solution based on the finite-difference method is obtained with the vorticity – stream function formulation. The results display the effects of the enclosure inclination angle and the Hartmann number for two different Rayleigh numbers on the contour maps of the streamlines and temperature. The results for the average Nusselt number are presented and discussed for various parametric conditions. Sivasankaran S., 2011 investigated numerically the convective flow and heat transfer characteristics of nanofluid in a two dimensional square cavity in the presence of uniform horizontal magnetic field. The vertical walls of the cavity are isothermal whereas the horizontal walls are adiabatic. The finite volume method is used to discretize the governing equations and solved by iterative technique. Two different models are considered for calculating the effective viscosity of the nanofluid. It is found that convection heat transfer is affected significantly in presence of horizontal magnetic field. A small change is observed in temperature field between two models when increasing the volume fraction and Hartmann number. When increasing the volume fraction of the nanofluid,

the heat transfer rate is increased monotonically for model I and decreased for model II for weak magnetic field, whereas heat transfer rate of both models increased for moderate and strong magnetic field.

Sheikholeslami et. al., 2013 investigated numerically the magnetic field effect on natural convection heat transfer in a curved-shape enclosure. The numerical investigation is carried out using the control volume-based-finite element method (CVFEM). The investigations are performed for various values of Hartmann number and Rayleigh number. The obtained results are depicted in terms of streamlines and isotherms which show the significant effects of Hartmann number on the fluid flow and temperature distribution inside the enclosure. Also, it was found that the Nusselt number decreases with an increase in the Hartmann number.

Parvin S. and Nasrin R., 2011 are used a finite element method based on Galerkin weighted Residual approach to solve two-dimensional governing mass, momentum and energy equations for steady state, natural convection flow in presence of magnetic field inside a square enclosure. The cavity consists of three adiabatic walls and one constantly heated wall. A uniformly heated circular solid body is located at the centre of the enclosure. The aim of this study is to describe the effects of MHD on the flow and thermal fields in presence of such heated obstacle. The investigations are conducted for different values of Rayleigh number (Ra) and Hartmann number (Ha). Various characteristics of streamlines, isotherms and heat transfer rate in terms of the average Nusselt number (Nu) are presented for different parameters. The results indicate that the flow pattern and temperature field are significantly dependent on the above mentioned parameters.

The study includes the numerical investigation of natural convection heat transfer from circular horizontal cylinder placed in a square enclosure. The investigation deals with the effect of magnetic field on the behavior of the flow and temperature distributions and Nusselt number using different Rayleigh numbers Ra, and various Hartman numbers.

Mathematical Formlation

The natural convection heat transfer between the horizontal cylinder and the enclosure are presented using governing equations, as shown in figure (1), Ali O. M., 2014. The flow are based on the following assumptions: the flow is incompressible, Boussinesq, no internal heat sources, laminar flow, and two-dimensional with take into account the effect of the magnetic field.

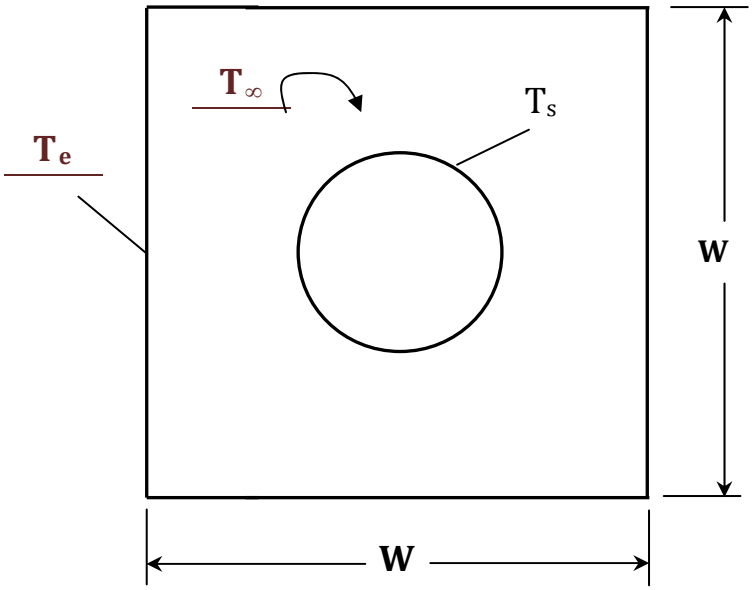

Figure (1): Configuration of cylinder-enclosure combination

The governing equations are presented as follows, Parvin S., and Nasrin R., 2011: Continuity equation:

$$\frac{\partial u}{\partial x}+\frac{\partial v}{\partial y}=0 \qquad (1)$$

The momentum equation in x-direction is:

$$\frac{\partial \mathrm{u}}{\partial \mathrm{t}}+\mathrm{u}\frac{\partial \mathrm{u}}{\partial \mathrm{x}}+\mathrm{v}\frac{\partial \mathrm{u}}{\partial \mathrm{y}}=-\frac{1}{\rho}\frac{\partial \mathrm{p}}{\partial \mathrm{x}}+\frac{\partial}{\partial \mathrm{x}}\left(\mu\frac{\partial \mathrm{u}}{\partial \mathrm{x}}\right)+\frac{\partial}{\partial \mathrm{y}}\left(\mu\frac{\partial \mathrm{u}}{\partial \mathrm{y}}\right) \qquad (2)$$

The momentum equation in y-direction is:

$$\frac{\partial \mathrm{v}}{\partial \mathrm{t}}+\mathrm{u}\frac{\partial \mathrm{v}}{\partial \mathrm{x}}+\mathrm{v}\frac{\partial \mathrm{v}}{\partial \mathrm{y}}=-\frac{1}{\rho}\frac{\partial \mathrm{p}}{\partial \mathrm{y}}+\frac{\partial}{\partial \mathrm{x}}\left(\mu\frac{\partial \mathrm{v}}{\partial \mathrm{x}}\right)+\frac{\partial}{\partial \mathrm{y}}\left(\mu\frac{\partial \mathrm{v}}{\partial \mathrm{y}}\right)+\mathrm{g}\dot{\beta}\Delta\mathrm{T}-\sigma\mathrm{B}_{\mathrm{o}}^{2}\upsilon \qquad (3)$$

The energy equation is:

$$\rho c\left(\frac{\partial T}{\partial t}+u\frac{\partial T}{\partial x}+v\frac{\partial T}{\partial y}\right)=\frac{\partial}{\partial x}\left(k\frac{\partial T}{\partial x}\right)+\frac{\partial}{\partial y}\left(k\frac{\partial T}{\partial y}\right) \qquad (4)$$

μ is laminar viscosity.

According to the Boussinesq approximations, the density is a linear function of the temperature. The buoyancy force term in the y-momentum equation.

$$\rho=\rho_o\left(1-\dot{\beta}\Delta T\right) \qquad (5)$$

Where β is the thermal expansion coefficient.

The stream function (ψ) and vorticity (ω) in the formulated governing equations may be defined in the following manner, Anderson, 1995 and Petrovic, 1996:

$$u=\frac{\partial \psi}{\partial y},\quad v=-\frac{\partial \psi}{\partial x} \qquad (6)$$

$$\omega=\frac{\partial v}{\partial x}-\frac{\partial u}{\partial y} \qquad (7)$$

Or $\omega=\nabla\times\vec{V}$

The governing equations are formulated as follows:

Energy Equation:

$$\frac{\partial \theta}{\partial t}+\frac{\partial \Psi}{\partial y}\frac{\partial \theta}{\partial x}-\frac{\partial \Psi}{\partial x}\frac{\partial \theta}{\partial y}=\left(\frac{\partial^2\theta}{\partial x^2}+\frac{\partial^2\theta}{\partial y^2}\right) \qquad (8)$$

Momentum Equation:

$$\frac{\partial \varpi}{\partial \mathrm{t}}+\frac{\partial \Psi}{\partial \mathrm{y}}\frac{\partial \varpi}{\partial \mathrm{x}}-\frac{\partial \Psi}{\partial \mathrm{x}}\frac{\partial \varpi}{\partial \mathrm{y}}=\mathrm{Pr}\left(\frac{\partial^2 \varpi}{\partial \mathrm{x}^2}+\frac{\partial^2 \varpi}{\partial \mathrm{y}^2}\right)+\mathrm{Ra}\ \mathrm{Pr}\frac{\partial \theta}{\partial \mathrm{x}}+\mathrm{Ha}^2\ \mathrm{Pr}\frac{\partial \Psi}{\partial \mathrm{x}} \qquad (9)$$

Continuity Equation:

$$\frac{\partial^2\Psi}{\partial x^2}+\frac{\partial^2\Psi}{\partial y^2}=-\varpi \qquad (10)$$

Where $Pr=\frac{\vartheta}{\alpha}$ is Prandtl number, $Ra=\frac{g\beta\Delta TL^3}{\vartheta\alpha}$ is Rayleigh number and Ha is the Hartman number which is defined as $Ha^2=\frac{\sigma B_o^2L^3}{\mu}$.

The variables are defined in the nondimensional forms in the governing equations:

$$X=\frac{x}{D},\quad Y=\frac{y}{D},\quad U=\frac{uD}{\vartheta},\quad V=\frac{vD}{\vartheta},$$

$$\tau=\frac{t\vartheta}{D^2},\quad \Psi=\frac{\psi}{\vartheta},\quad \varpi=\frac{\omega D^2}{\vartheta},\quad \theta=\frac{\mathrm{T}-\mathrm{T}_\infty}{\mathrm{T}_c-\mathrm{T}_\infty} \qquad (11)$$

The characteristic length in the governing equations is the cylinder diameter D. By using dimensionless parameters, the equations (8)-(10) transformed into general form for the computational space:

$$a_\phi\left\{\frac{\partial\phi}{\partial t}+\frac{1}{J}\left[\left(\frac{\partial\psi}{\partial\eta}\phi\right)_\xi-\left(\frac{\partial\psi}{\partial\xi}\phi\right)_\eta\right]\right\}=\nabla\left(b_\phi\nabla\phi\right)+d_\phi \qquad (12)$$

Where ϕ the dependent variable.

The three governing equations may be defined by changing the dependent variable ϕ as follow

ϕ	a_ϕ	b_ϕ	d_ϕ
ψ	0	1	ω
ω	1	μ	$\frac{g\beta}{J}\left[(y_\eta\theta)_\xi-(y_\xi\theta)_\eta\right]+\frac{Ha^2}{J^2}\left[(y_\eta\Psi)_\xi-(y_\xi\Psi)_\eta\right]$
T	1	μ/k	0

$\frac{\partial\phi}{\partial t}$ is the unsteady term.

$\frac{1}{J}\left[\left(\frac{\partial\psi}{\partial\eta}\phi\right)_\xi-\left(\frac{\partial\psi}{\partial\xi}\phi\right)_\eta\right]$ is the convective term.

$\nabla(b_\phi\nabla\phi)$ is the diffusion term.

And the d_ϕ is the source term.

Grid Generation

The initial computational grid generation is obtained using algebraic grid generation method. The second step, include using elliptic partial differential equations (Poisson equations) to generate grid points, Ali O. M., 2014:

$$\xi_{xx}+\xi_{yy}=P(\xi,\eta) \qquad (13a)$$

$$\eta_{xx}+\eta_{yy}=Q(\xi,\eta) \qquad (13b)$$

By interchanging dependent and independent variables for equations (13a, and b), gives:

$$\alpha x_{\xi\xi}-2\beta x_{\xi\eta}+\gamma x_{\eta\eta}+J^2\left(P x_\xi+Q x_\eta\right)=0 \qquad (14a)$$

$$\alpha y_{\xi\xi}-2\beta y_{\xi\eta}+\gamma y_{\eta\eta}+J^2\left(P y_\xi+Q y_\eta\right)=0 \qquad (14b)$$

Where $\alpha=x_\eta^2+y_\eta^2$; $\beta=x_\xi x_\eta+y_\xi y_\eta$;

$\gamma=x_\xi^2+y_\xi^2$

The choice of the coordinate control functions P and Q are important due to its effect on the structure of the grid, Thomas et. al., 1980. The successive over Relaxation (SOR) method with relaxation factor value equal to 1.4 is used to solve the elliptic partial differential equations, Hoffman, 1989 and Thompson, 1985.

The computational domain using elliptic grid generation is shown in figure (2).

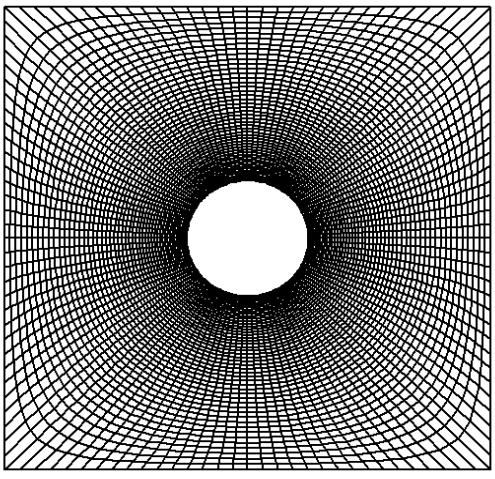

Figure (2): Transformations of the physical domains into computational domains using elliptic grid generation.

Method of Solution

The numerical investigation include conversion of the governing equations into algebraic equations, by the use of a Finite Volume based Finite Difference method using Fortran language, Ferziger, 2002.

The hybrid scheme of the central differencing scheme and the upwind differencing scheme is employed. This method is used to avoid the instability of the central differencing scheme at high Peclet number (Cell Reynolds Number) and an inaccuracy of the upwind differencing scheme.

$$a_P \phi_P = a_E \phi_E + a_W \phi_W + a_N \phi_N + a_S \phi_S + a_P^o \phi_P^o + a_M \left(\phi_{i+1,j+1} - \phi_{i-1,j-1} - \phi_{i+1,j-1} + \phi_{i-1,j+1}\right) + d_{i,j} \quad (15)$$

$$a_P = a_E + a_W + a_N + a_S + a_P^o \quad (16)$$

The alternating direction method ADI is used to solve the resulting algebraic equation. The ADI method includes two sweeps; in the first sweep, the equations are solved implicitly in ξ-direction using Cyclic TriDiagonal Matrix Algorithm (CTDMA) because of its cyclic boundary conditions and explicitly in η-direction. In the second sweep, the equations are solved implicitly in η-direction by using TriDiagonal Matrix Algorithm (TDMA) and explicit in ξ-direction.

Successive Over-Relaxation method (SOR) is used to solve the stream function equation.

The flow between heated cylinder and enclosure have the following initial conditions:

$\Psi=0, \theta = 0, \omega = 0$ For t = 0 (17)

The boundary condition of the temperature for cylinder surface is:

$\theta = 0$ (18)

The boundary conditions of the vorticity, Roache, 1982, are

$$\varpi = \frac{2\gamma}{J^2}\left(\psi_{i,m} - \psi_{i,m-1}\right) \quad \text{at enclosure wall} \quad (19a)$$

$$\varpi = \frac{2\gamma}{J^2}\left(\psi_{i,1} - \psi_{i,2}\right) \quad \text{at cylinder surface} \quad (19b)$$

The cylinder stream function is constant and equal to zero. The stream function of the enclosure is constant.

The Nusselt number Nu is a measure to determine the enhancement of the heat transfer that calculated using the following formula:

$$Nu = \frac{\sqrt{\gamma}}{J}\int_0^{2\pi} \frac{\partial\theta}{\partial\eta} d\zeta \quad (20a)$$

The following formula is used to calculate the derivative of the nondimensional temperature, Fletcher, 1988 :

$$\left.\frac{\partial\theta}{\partial n}\right|_{\eta=const.} = \frac{1}{J\sqrt{\gamma}}\left(-\beta\theta_\xi + \gamma\theta_\eta\right) = \frac{\sqrt{\gamma}}{J}\frac{\partial\theta}{\partial\eta} \quad (20b)$$

$\theta_\xi = 0$ at cylinder surface

The execution of the numerical algorithm is based on the Fortran language. The computer program is general for a natural convection from heated cylinder placed in a squnre enclosure.

Results and Discussion

The numerical study deals with natural convection heat transfer from circular horizontal cylinder when housed in an enclosed square enclosure in the presence of the magnetic field. The investigation uses constant aspect ratios W/D = 2.5, different Rayleigh numbers of 10^3, 10^4, and 10^5 and different Hartman numbers of 0, 50, 100, and 200.

The numerical results that solved by ADI method become convergent when temperature T, stream function ψ and vorticity ω reach to the convergence criteria as $R_T<10^{-6}$, $R_\psi<10^{-6}$ and $R_\omega<10^{-6}$ and the results will be obtained.

Stability and Grid Independency Study

Three time steps will be chosen for the case $Ra=10^5$, W/D=2.5, Pr = 0.7. The time steps values are 1×10^{-4}, 5×10^{-4}, 5×10^{-6}. The maximum difference between the values of the Nusselt numbers is reasonable ~about 2%.

The numerical results are compared for three mesh sizes of 96×25, 128×45, and 192×50 to test the grid-independence. The numerical results showed that the optimum mesh size is 128×45 that used in the study for all cases.

Validation Test

The present numerical results are compared with the previous numerical results of the Moukalled and Acharya, 1996. The comparisons was made for average Nusselt numbers and maximum stream function ψ_{max} for the case of enclosure width to cylinder diameter ratios (W/D=1.667, 2.5, and 5), Rayleigh numbers $Ra=10^4$ and 10^5 as given in table (1). The results, that shown in table (1), indicated a good agreement between two results.

Table (1): Comparisons of Nusselt numbers and maximum stream function with previous data.

L/D	Ra	ψ_{max}		$\overline{Nu}$	
		Present	Moukalled and Acharya, 1996	Present	Moukalled and Acharya, 1996
5.0	10^4	2.45	2.08	1.7427	1.71
2.5		3.182	3.24	0.9584	0.97
1.67		5.22	5.4	0.4274	0.49
5.0	10^5	10.10	10.15	3.889	3.825
2.5		8.176	8.38	4.93	5.08
1.67		4.8644	5.10	6.23	6.212

Flow and Temperature Patterns

The natural convection heat transfer from circular cylinder in an enclosure in the presence of the magnetic fluid is investigated numerically using finite difference method. The study include various values of Rayleigh numbers, Ra= 10^3, 10^4, and 10^5, Hartman number values Ha = 0, 50, 100, and 200 with Prandtl number, Pr = 0.7.

The flow and temperature patterns are displayed in figures (3-5). Figure (3) show the streamlines and isotherms for Ra = 10^3. The isotherms display as rings around the circular cylinder for all Hartman numbers. The above trends ensure that the conduction heat transfer is the dominant mode. The flow distributions for Ha = 0 and Ha = 50 are similar and the eddies appear as a curved kidney-shaped contain two kernel eddies for each side. The maximum stream function, as a measure of the intensity of the natural convection in the enclosure, for Ha =0 is Ψ_{max}= 0.0882 and its value reduces to Ψ_{max} = 0.00312 for Ha = 50. The flow of the two cases is symmetrical about its vertical line through the center of the circular cylinder. The main eddies

distort at Ha = 100 and the flow become more condense. Four tiny nearly circular shaped appear at the corners of the enclosure. Also the flow is nearly symmetrical about the vertical line through the center of the circular cylinder. The maximum stream function decreases to Ψ_{max} = 0.0008426**.** As Hartman number increases to Ha = 200, the flow becomes weak and the maximum stream function drop to Ψ_{max} = 0.0002192. The flow is nearly symmetrical and the eddies become less dense. The four tiny sub eddies becomes large and display as kernel-shaped.

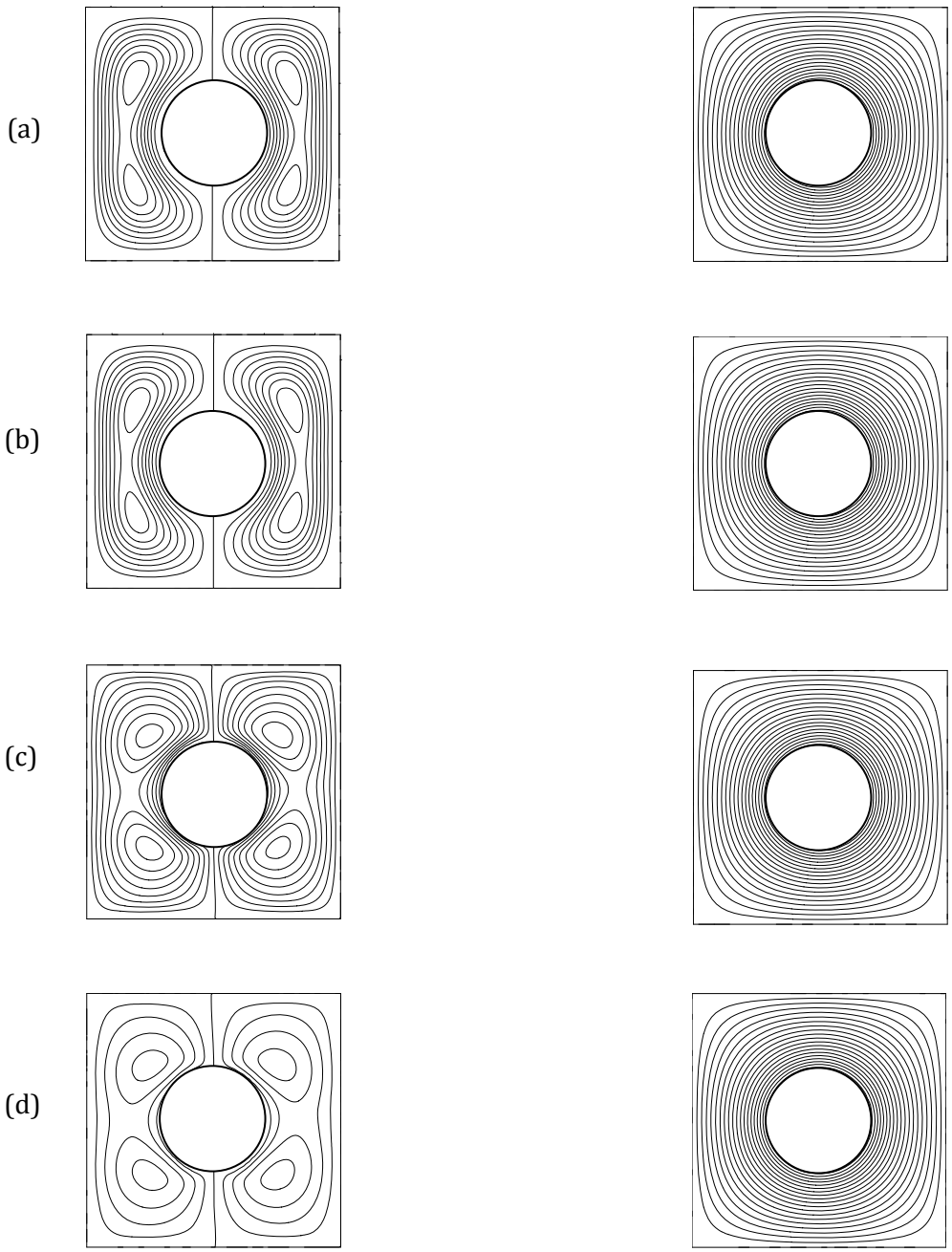

Figure (3): Effect of Hartman number on streamlines at W/D = 2.5 and Ra = 10^3 for (a) Ha = 0, (b) Ha = 50, (c) Ha = 100, (d) Ha = 200.

The characteristics of the flow and temperature distributions for Ra = 10^4 appear in figure (4). The isotherms for all Hartman numbers display as those for Ra = 10^3 and appear as rings around the circular cylinder that ensure the domination of the conduction heat transfer. The flow for Ha = 0 is symmetrical about the vertical line through the center of the circular cylinder. The eddies appear as curved kidney-shaped around the cylinder. The maximum stream function increases, as compared with Ra = 10^3, and becomes Ψ_{max} = 0.469. A tiny kernel-shaped eddy display in each main eddy. The flow for Ha = 50 display nearly symmetrical about the vertical line. The flow becomes weak and the maximum stream function reduces to Ψ_{max} = 0.03045. The main eddies become more dense and three tiny eddies appear at the corners of the enclosure. For Ha = 100, the eddies become more dense and cover most of the space between the cylinder and the enclosure. The number of tiny eddies at the corners of the enclosure is four. The flow is weaker and the maximum stream function reduces to Ψ_{max} = 0.00831. As influence of the magnetic field becomes more and the Hartman number increases to Ha = 200, the flow becomes more dense and cover all the space between the cylinder and the enclosure and the eddies distort and asymmetrical about the vertical line. The maximum stream function drops to Ψ_{max} =0.002174.

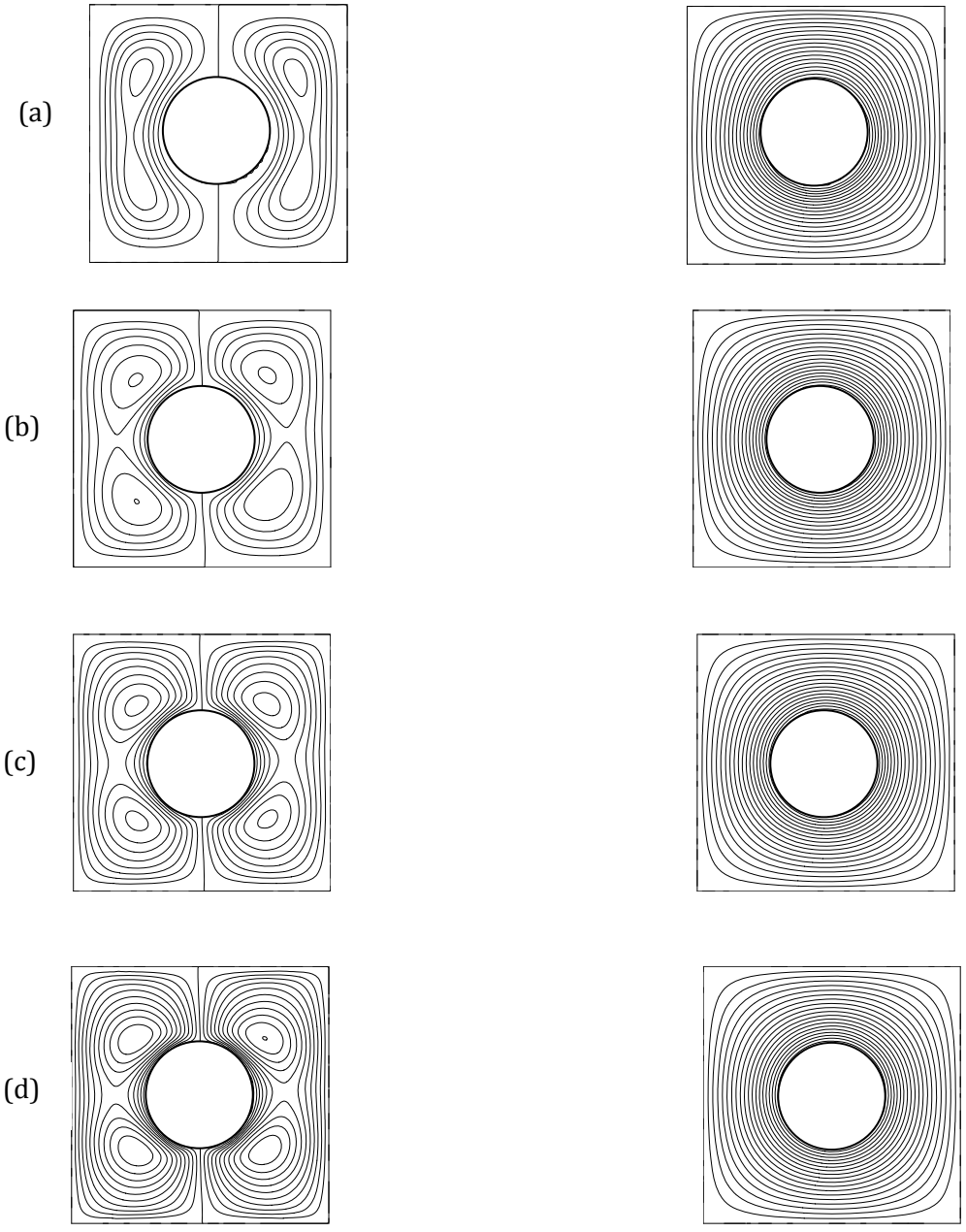

Figure (4): Effect of Hartman number on streamlines at W/D = 2.5 and Ra = 10^4 for (a) Ha = 0, (b) Ha = 50, (c) Ha = 100, (d) Ha = 200.

The aspects of the flow and temperature distributions for Ra = 10^5 are displayed in figure (5). The isotherms for Ha = 0, in absence of the magnetic field, verify the natural convection heat transfer is the dominant mode. A main thermal plume appears above the circular cylinder with two thermal plumes at the sides of the main thermal plume. The mode of the heat transfer becomes conduction for other Hartman numbers due to the effect of the magnetic field as displayed from temperature distributions that appear as rings around the cylinder.

For streamlines at Ha = 0, the maximum stream function increases with the increase of the Rayleigh number and its value becomes Ψ_{max} = 8.175 due to the effect of the natural convection. The eddies display as curved kidney-shaped contain one tiny circular-shaped eddy for each main eddy. As Hartman number increases to Ha =50, the eddies distort and the flow become asymmetrical about the vertical line. The maximum stream function decreases to Ψ_{max} = 0.2963. Four unequal large sub eddies appear at the corners of the enclosure. At Ha = 100, the flow becomes more orderly and become nearly symmetrical about the vertical line through the center of the circular cylinder. The flow becomes more dense and cover all the space between the cylinder and the enclosure. The maximum stream function decreases to Ψ_{max} = 0.084087. for Ha = 200, the flow become less dense and symmetrical about the vertical line through the center of the cylinder. With appearance of four equal sub eddies at the corners of the enclosure. The maximum stream function becomes Ψ_{max} = 0.02193.

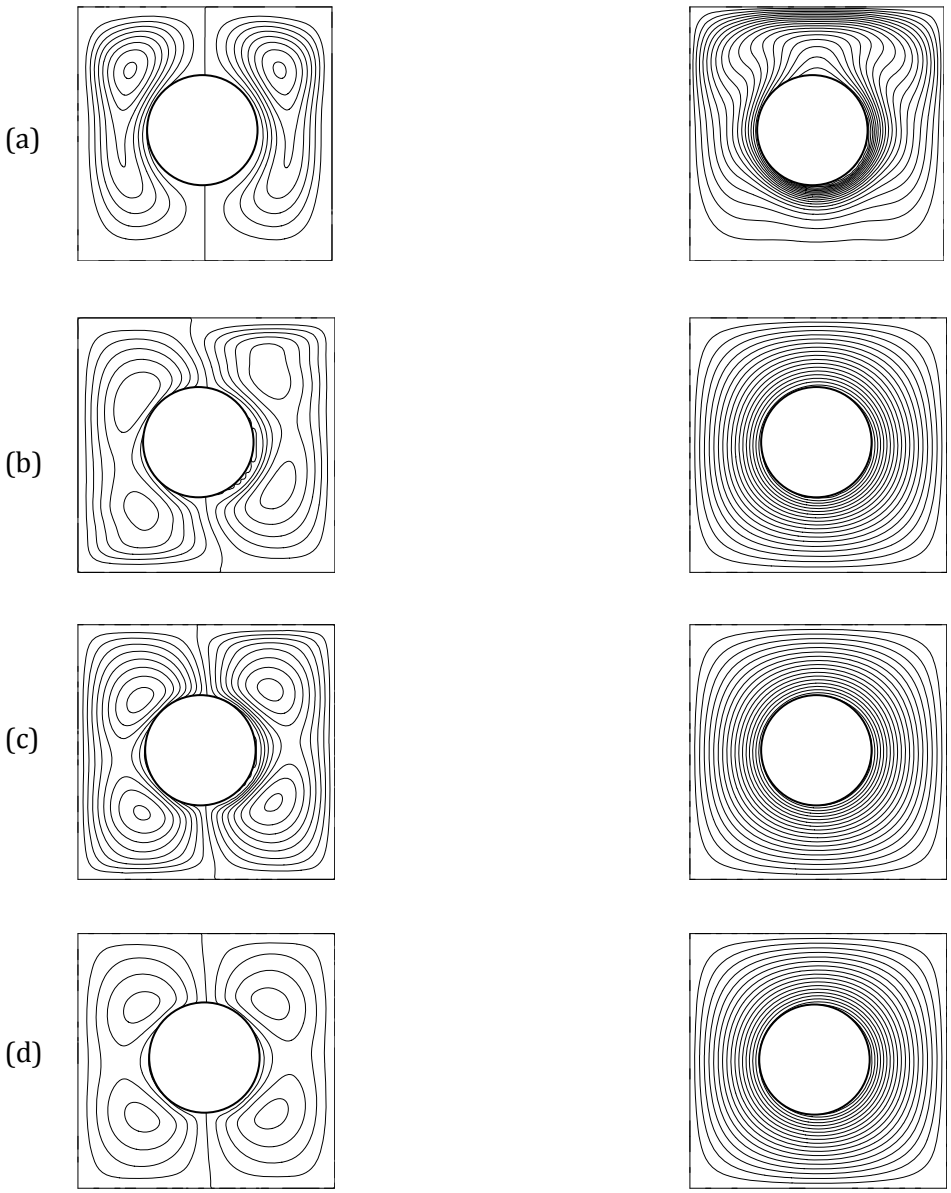

Figure (5): Effect of Hartman number on streamlines at W/D = 2.5 and Ra = 10^5 for (a) Ha = 0, (b) Ha = 50, (c) Ha = 100, (d) Ha = 200.

Local and Overall Heat Transfer Coefficients

The investigation of heat transfer from circular cylinder is presented by the Nusselt number. The effect of magnetic field on the local and overall Nusselt numbers with Ra=10^3, 10^4, 10^5 for enclosure width to the cylinder ratio W/D= 2.5 are presented in figures (6-9). The Hartman numbers in the investigation are: 0, 50, 100, 200. The local Nusselt number is measured from the center of the right side of the cylinder ($\theta = 0°$) and return to the same point ($\theta = 360°$). The local Nusselt numbers for Ra = 10^3 are displayed in figure (6). The local Nusselt numbers are identical for Ha > 0. The aspects of the local Nusselt number in absence of the magnetic field is different from those in presence of the magnetic field. For $\theta < 180°$, the local minimum and maximum values of the local Nusselt numbers for Ha = 0 are less than those for other Hartman numbers. For $\theta > 180°$, the local minimum and maximum values of the local Nusselt numbers for Ha = 0 are more than those for other Hartman numbers. At Ra = 10^4, as shown in figure (7), the local Nusselt number for Ha = 0 decreases with increasing the inclination angle and reach a minimum value at $\theta \approx 90°$, then the local Nusselt number increases reaching maximum value at $\theta \approx 280°$ and decreases to the initial value of the local Nu. For other values of the Hartman numbers, the aspects of the local Nusselt number are different. There are three similar sections for local Nu behavior. For each section, the local Nu begin with high value and decreases to low value then return to the same high value. For Ra = 10^5, as shown in figure (8), the local Nusselt number begin from high value at right side $\theta = 0°$. It decreases to minimum value above the cylinder $\theta = 90°$, then increases to maximum value below the cylinder $\theta = 270°$. The local Nusselt number returns to initial value at $\theta = 0°$. The behavior of local Nusselt number for Ha = 50 is similar but with low values. The minimum and maximum local Nusselt number positions are same with low values. The values of the local Nusselt numbers are approximately constant due to the effect of the Lorentz force (magnetic field).

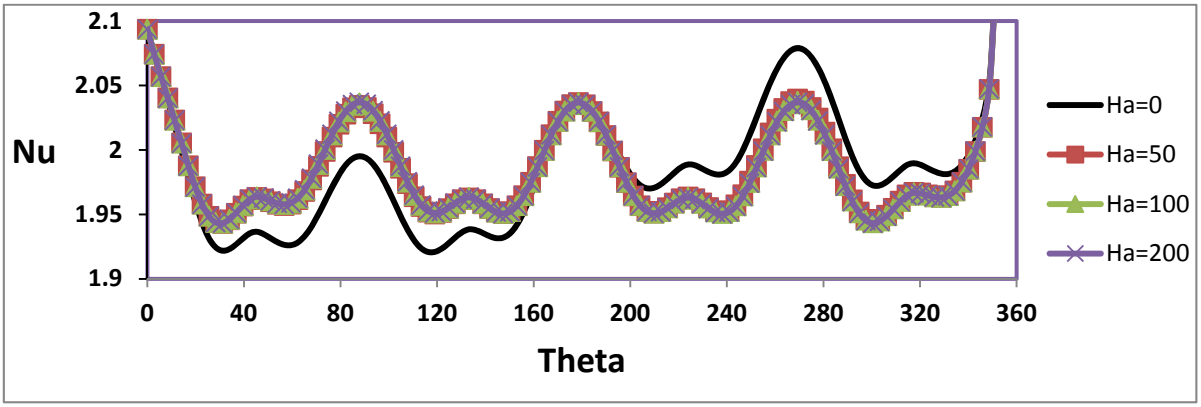

Figure (6): Effect of Hartman number on the local Nusselt number for Ra = 10^3.

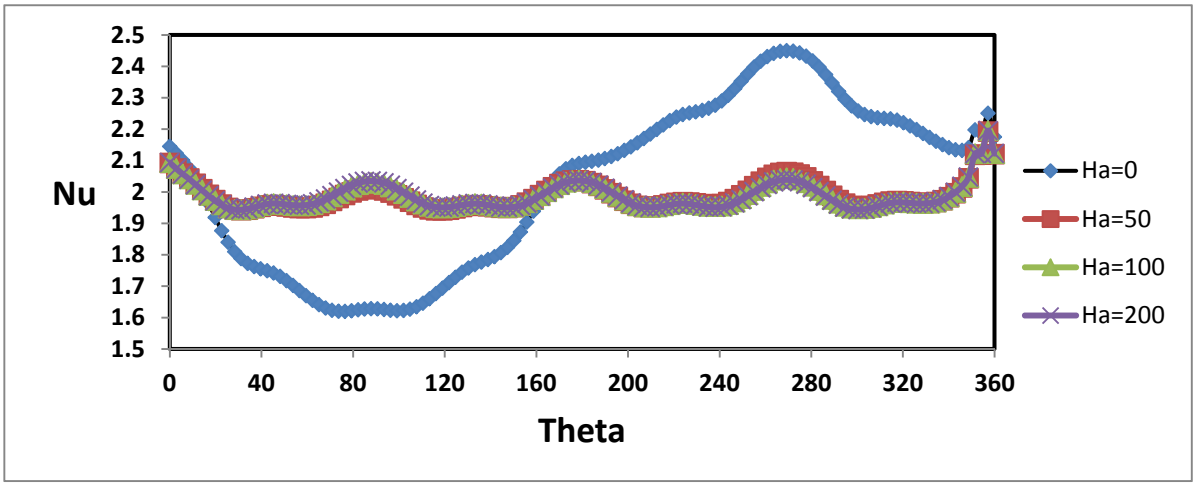

Figure (7): Effect of Hartman number on the local Nusselt number for Ra = 10^4.

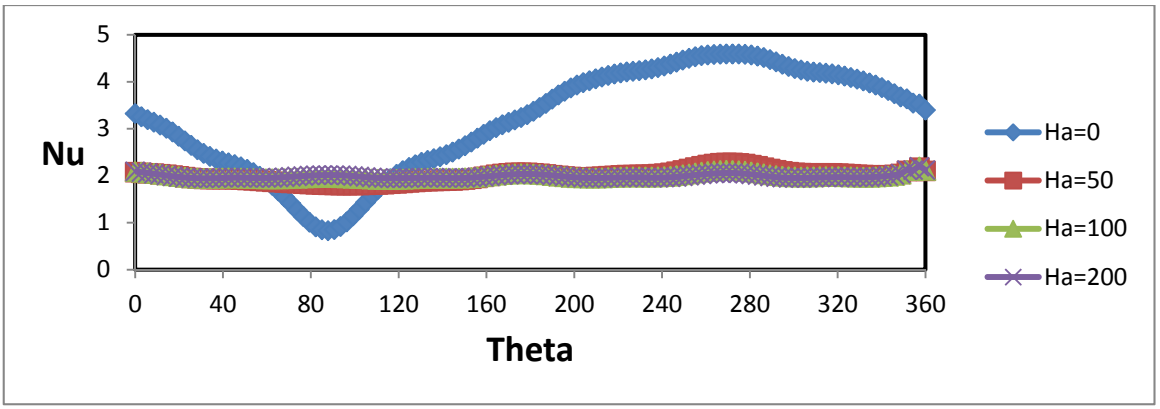

Figure (8): Effect of Hartman number on the local Nusselt number for Ra =

The effect of the Hartman number variation on the average Nusselt number is displayed in figure (9). At Ra=10^3, the Nusselt number remain constant for all Hartman numbers that the mode of heat transfer is conduction. At Ra=10^4, the Nusselt number decreases slightly for Ha =50 and remain constant for other Hartman numbers because the mode of the heat transfer convert to the conduction. At Ra=10^5, the natural convection heat transfer is the dominant mode for Ha= 0. The conduction mode become the domination mode for other Hartman numbers due to the effect of the magnetic field in the fluid.

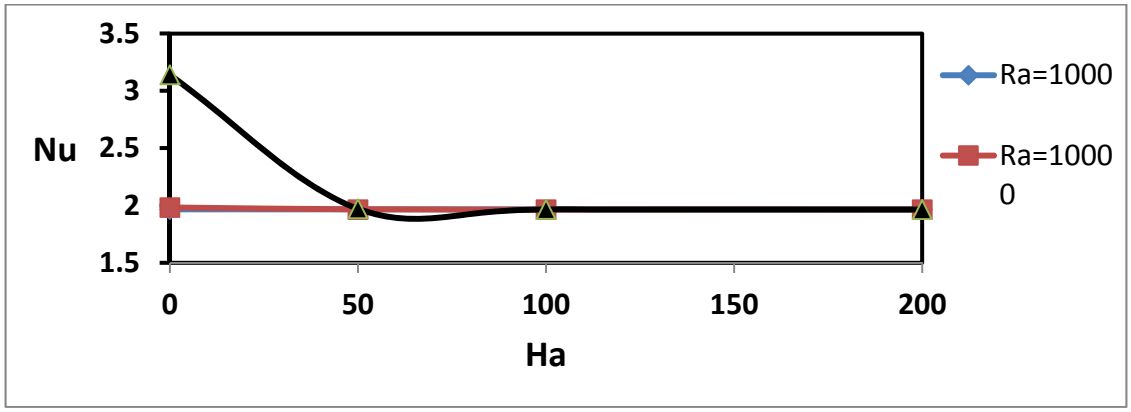

Figure (9): Effect of Hartman number on the average Nusselt number for W/D=1.67.

Conclusions

Effect of Hartman number on the natural convection heat transfer from circular horizontal cylinder in a square enclosure was investigated numerically over a fairly wide range of Ra. The main conclusions of the present work can be summarized as follows:

1. The numerical results show that the Nusselt number increases with increasing the Raylieh number for all cases.
2. The flow patterns and isotherms display the effect of Ra and Hartman number on the thermal and hydrodynamic characteristics.
3. The results show that the conduction heat transfer is the dominant mode for low Rayleigh numbers.
4. The convection heat transfer is the dominant mode of the heat transfer for high Rayleigh number in absence of the magnetic effect.
5. The magnetic field in the fluid, that represents by the Hartman number, convert the convection heat transfer to conduction mode for high Rayleigh numbers.
6. The results show that the behavior of the local Nusselt numbers for Ha = 0 are unique and differ from those of other higher Hartman numbers for all Rayleigh numbers.

References

Ali Al-Mudhaf, Ali J. Chamkha, (2004). Natural convection of liquid metals in an inclined enclosure in the presence of a magnetic field. International Journal of Fluid Research. Vol. 31, No. 3, pp. 221-243.

Ali O. M. (2008), "Experimental and Numerical Investigation of Natural Convection Heat Transfer From Cylinders of Different Cross Section Cylinder In a Vented Enclosure," Ph. D., Thesis, College of Engineering, University of Mosul.

Ali O. M., (2014). Numerical Investigation of Prandtl Number Effects on the Natural Convection Heat Transfer From Circular Cylinders In an Enclosed Enclosure. Journal of University of Zakho, A-Science, Vol. 2, No. 2, pp. 358-374.

Bejan A. and Kraus A. D., (2003). Heat Transfer Handbook. John Wiley & Sons, Inc., Hoboken, New Jersey.

Ferziger J. H. and Peric M., (2002). Computational Methods for Fluid Dynamics. Springer, New York.

Fletcher C.,A.,J., (1988). Computational Techniques for Fluid Dynamics 2. Springer, Verlag.

Hoffmann K. A., (1989). Computational Fluid Dynamics For Engineers. Engineering Education System, USA.

John D. Anderson Jr., (1995). Computational Fluid Dynamics, the Basics with Applications. McGraw–Hill Book Company.

Kuehn TH, Goldstein RJ., (1976). An experimental and theoretical study of natural convection in the annulus between horizontal concentric cylinders. Journal of Fluid Mechanics, Vol. 74, pp. 695–719.

Moukalled F., Acharya S., (1996). Natural convection in the annulus between concentric horizontal circular and square cylinders. Journal of Thermophysics and Heat Transfer; Vol. 10(3), pp. 524 –531.

Parvin S., Nasrin R., (2011). Analysis of the flow and heat transfer characteristics for MHD free convection in an enclosure with a heated obstacle. Nonlinear Analysis Modeling and Control. Vol. 16, No. 1, pp. 89-99.

Petrović Z., and Stupar S., (1996). Computational Fluid Dynamics, One. University of Belgrade.

Roache, P., J., (1982). Computational Fluid Dynamics. Hermosa publishers.

Sheikholeslami M., Hashim I., Soheil Soleimani, (2013). Numerical investigation of the effect of magnetic field on natural convection in a curved-shape enclosure. Mathematical Problems in Engineering. Vol. 2013, Article ID831726.

Shu C.; and Y. D. Zhu, (2002). Efficient computation of natural convection in a concentric annulus between an outer square cylinder and an inner circular cylinder. International Journal For Numerical Methods In Fluids, Vol. 38, pp. 429-445.

Sivasankaran S., (2014). Natural convection of nanofluids in a square cavity in the presence of horizontal magnetic field. International Conference Data Mining, Civil, Mechanical Engineering (ICDMCME2014); Feb. 4-5, Bali (Indonesia).

Taghikhani M.A., Najafkhani H., (2013). Investigation of magnetic field effect on natural convection using fast Ψ-Ω method. International Research Journal of Applied and Basic Sciences, Vol. 4, No. 10, pp. 2939-2949.

Thomas P. D., and Middlecoff J. F., 1980. Direct Control of the Grid Point Distribution in Meshes Generated by Elliptic Equations. AIAA Journal, Vol. 18, No. 6, pp. 652-656.

Thompson J. F., Warsi Z. U. A. and Mastin C. W., (1985). Numerical Grid Generation: Foundations and Applications. Mississippi State, Mississippi.

خواندنا تیوری ب ئامادەبوونا کاریگەری موگناتیسی لسەر ڤەکوهاستنا گەرماتیی ل لولەك دەرژکەری بە شیوەکی بازنەیی ل کورەکی کەرتی

کورتیا لێکولینێ:

دڤی ڤەکولینی بخو فە گریدایە ب خواندنا تیوری بو ڤەکوهاستنا گەرماتیی ژ باراکی سەروشتی ل لولەك دەرژکەری بە شیوەکی بازنەیی ل کورەکی کەرتی. ئەف شولا دیاردەکیت تیستەکی ژ گرەنگیا گوهورینا ژماریت هارتمان (0، 50، 100، 200)، ژماریت رایلی (10^3، 10^4، و10^5) دگەل ریژی ستیرادیت کورەکی بو تیرەی بازنە یا لولەکی W/D یەکسان بو 2.5. شولێ تیوری بیکتیت ژ شیکارکەرنا هاوکیشییت جیاکاریانە دادەریژیت فورتیسیق–ئیشییت جوگە وهاتە گهورین بو سیستەمی ریکیەخات ییت دەکونجیت بو لاشی. هاتە بکارئینان بو جارا ئیگی ریگە جەبری بو وەچە توێرێ ژ بەر نواندنا ناوچە فیزیاوی نێوان لوولەکا ئاسۆیی و کلۆرێ داخراو . باشی هاتە دووبارە کردنەوە وەچە توێرێ بریگە جیاکاریانە بەشی. هاتە بکارئینان ریگە جیاوازی دیاریکراو بو شیکارکەرنا سیستەمی هاوکیشییت جیاکاریانە.

ڤی ڤەکولینی هاتا دیارکرن گرنگیا گهورینا ژماریت هارتمان ل سەر ژمارا نسلت یی شوینی وتیکرایی، هێلێت ڕێڕەو، وهێلێت پلای گەرماتیی دەڤ ژمارییت رایلی جیاواز. دیارکری شوینەواری ژمارییت هارتمان ل سەر هێلێت ڕێڕەو، وهێلێت پلای گەرماتیی بریکا نووسین دەروات ونووسینی پلا گەرماتیی.

ئەنجامییت ڤەکولینی دیارکر کو گواستنەوە گەرماتی بە گەیاندن زوردار دەف ژمارییت رایلی ییت نزم. گواستنەوە گەرماتی بە هەلگرتنی زوردار دەف ژمارییت رایلی ییت بلند بە نە ئامادەبوونا کاریگەری موگناتیسی. گواستنەوە گەرماتی بە هەلگرتنی دەگوریت بو گواستنەوە گەرماتی بە گەیاندن دەف ژمارییت رایلی ییت بلن دبە ئامادەبوونا کاریگەری موگناتیسی ل شلاتی. ئەنجامییت ڤەکولینی دیارکر کو ژمارییت نسلت یی شوینی دەف ژمارا هارتمان یەکسان بو چنە رەفتارەك بتنی هەیە جیاواز ژ ژمارییت نسلت یی شوینی دەمی ژمارییت هارتمان بلندبییت بو هەمی ژمارییت رایلی.

دراسة عددية لتأثير المجال المغناطيسي على انتقال الحرارة بالحمل الطبيعي من اسطوانة دائرية في حيز مغلق

الملخص:

يبحث العمل الحالي فحص عددي لانتقال الحرارة بالحمل الطبيعي من اسطوانة دائرية افقية موضوعة في تجويف مغلق. ويتناول البحث تأثير المجال المغناطيسي على خصائص الجريان وانتقال الحرارة. يستخدم الدراسة اعداد هارتمان مختلفة (0، 50، 100، 200)، اعداد رايلي مختلفة (10^3، 10^4، و10^5) ونسبة ثابتة لعرض التجويف الى قطر الاسطوانة W/D مساويا الى 2.5. الحل العددي يتضمن حلا للمعادلات التفاضلية في صيغة الدوامية–دالة الجريان والمتحولة إلى نظام إحداثيات المطابقة للجسم. استخدمت الطريقة الجبرية للتوليد الشبكي بشكل مبدئي لتمثيل المنطقة الفيزيائية الواقعة بين الاسطوانة الأفقية الساخنة والحيز المغلق وتم إعادة التوليد الشبكي باستخدام الطريقة التفاضلية الجزئية. استخدم طريقة الفروق المحددة لحل نظام المعادلات التفاضلية.

تم دراسة تأثير تغيير اعداد هارتمان على اعداد نسلت الموقعي والمتوسط، مقاطع الجريان وتوزيع درجات الحرارة عند اعداد رايلي مختلفة. ويظهر تأثير اعداد هارتمان عل مقاطع الجريان وتوزيع درجات الحرارة عن طريق استخدام خطوط الجريان وخطوط درجات الحرارة.

اظهرت النتائج بأن انتقال الحرارة بالتوصيل هو المتحكم عند اعداد رايلي المنخفضة. انتقال الحرارة بالحمل هو المتحكم عند اعداد رايلي المرتفعة عند عدم وجود التأثير المغناطيسي. يتحول انتقال الحرارة بالحمل الى انتقال الحرارة بالتوصيل عند اعداد رايلي عالية بوجود تأثير المجال المغناطيسي في المائع. اظهرت النتائج ان اعداد نسلت الموقعي عندما يكون عدد هارتمان مساوي لصفر له تصرف منفرد ومختلف عن اعداد نسلت الموقعي عندما يكون اعداد هارتمان عالية لكل اعداد رايلي.